Infrared Physics & Technology xxx (2014) xxx–xxx

Contents lists available at ScienceDirect

Infrared Physics & Technology

journal homepage: www.elsevier.com/locate/infrared

# Room temperature performance of mid-wavelength infrared InAsSb nBn detectors

Alexander Soibel *, Cory J. Hill, Sam A. Keo, Linda Hoglund, Robert Rosenberg, Robert Kowalczyk, Arezou Khoshakhlagh, Anita Fisher, David Z.-Y. Ting, Sarath D. Gunapala

*Jet Propulsion Laboratory, California Institute of Technology, 4800 Oak Grove Dr., Pasadena, CA 91030, United States*

## HIGHLIGHTS

- High temperature performance of MWIR nBn detectors was investigated.
- The quantum efficiency does not change with temperature between 77 and 325 K.
- Detector detectivity is $D^*(\lambda) = 1 \times 10^9$ (cm Hz$^{0.5}$/W) at $T = 300$ K.
- Detectors have potential for room temperature operation.

## ARTICLE INFO

*Article history:*
Received 22 July 2014
Available online xxxx

*Keywords:*
Infrared detectors
Semiconductor detectors
BIRD detectors
Sb-based detectors

## ABSTRACT

In this work we investigate the high temperature performance of mid-wavelength infrared InAsSb–AlAsSb nBn detectors with cut-off wavelengths near 4.5 µm. The quantum efficiency of these devices is 35% without antireflection coatings and does not change with temperature in the 77–325 K temperature range, indicating potential for room temperature operation. The device dark current stays diffusion limited in the 150–325 K temperature range and becomes dominated by generation-recombination processes at lower temperatures. Detector detectivities of $D^*(\lambda) = 1 \times 10^9$ (cm Hz$^{0.5}$/W) at $T = 300$ K and $D^*(\lambda) = 5 \times 10^9$ (cm Hz$^{0.5}$/W) at $T = 250$ K, which is easily achievable with a one stage TE cooler.



During the last several decades great efforts were dedicated to the development of high operating temperature infrared detectors for applications in imaging and chemical sensing [1]. A number of novel semiconductor devices, which rely on the suppression of thermal currents and an enhancement in responsivity to improve high temperature performance, have been proposed and realized [2]. Innovative detector architectures such as barrier structures, in particular nBn [3], devices and significant improvement in the performance GaSb-based alloys and superlattices [4] offer pathways to further improve high temperature operation.

The nBn, or more generally, XBn [5] device architecture differs from commonly used p–n junction by relying on a unipolar barrier to block majority carrier transport. Fig. 1 shows an energy diagram of a typical nBn detector that has an n-doped top contact, a barrier, and a lightly n-doped infrared absorber region. The barrier is designed such that it can block one carrier type (electrons in this case) but at the same time allow the unimpeded flow of the other (holes in this case). This is called a "unipolar" barrier. An important fact to note is that the barrier does not block the flow of photo-generated electrons or holes in the absorber, and therefore the signal (photocurrent) level is not affected. The nBn structure is designed to suppress the Shockley–Read–Hall (SRH) process generation-recombination (g–r) rate. Under operating conditions, the nBn structure is biased slightly for hole collection at the top contact. Most of the applied bias drops over the barrier region, for which the SRH dark current is almost totally suppressed because of the much wider band gap of the barrier. This is because the SRH processes are characterized by an activation energy of half band gap, $E_G/2$, and SRH related g–r dark current is proportional to, which is suppressed when is large. Surface leakage currents could also be suppressed in the nBn structure by fabricating nBn detectors in such a way that only the wide band gap barrier is exposed by shallow etching.

There has been rapid progress in the development of nBn devices which has resulted in the demonstration of single pixel and imagers based on InAs–AlAsSb, InAsSb–AlAsSb and InAs/GaSb–AlAsSb absorber–barrier material pairs, grown on InAs, GaSb

* Corresponding author at: JPL, 4800 Oak Grove Drive, M/S 302-205, Pasadena, CA 91109, United States. Tel.: +1 818 393 0225.

http://dx.doi.org/10.1016/j.infrared.2014.09.030
1350-4495/© 2014 Published by Elsevier B.V.

and GaAs substrates and covering both the mid-wavelength and long-wavelength infrared (MWIR and LWIR) spectral ranges [6–11]. However, until now the studies of these devices were hitherto limited to cryogenic temperatures.

We have recently investigated the high temperature performance of MWIR nBn InAsSb–AlAsSb detectors and demonstrate their potential for ambient temperature operation [12]. We observe that the responsivity of these detectors does not decrease for temperatures up to 325 K. Dark current at operational bias was found to stay diffusion limited in the 175–325 K temperature range and become dominated by generation–recombination (g–r) processes at lower temperature. This observed temperature dependence of dark current indicates an absence of surface leakage current, which typically has very weak temperature dependence, even in the fully pixelated, unpassivated detectors studied here [13]. The nBn detectors with cutoff wavelength near 4.5 μm demonstrated in this work exhibit a detectivity of $D^*(\lambda) = 5 \times 10^9$ (cm $Hz^{0.5}$/W) at $T = 250$ K, which is easily achievable with one stage TE coolers, and a $D^*(\lambda) = 1 \times 10^9$ (cm $Hz^{0.5}$/W) at $T = 300$ K. These results advance our understanding of high temperature operation of nBn detectors and will enable further improvement of these devices.

Fig. 1 shows the growth sequence and the energy band diagram of the nBn photodetector, whose absorber region consists of a 2 μm thick $InAs_{0.915}Sb_{0.085}$ absorber followed by a 0.1 μm $AlAs_{0.1}Sb_{0.9}$ barrier. The device structure was grown in a Veeco Applied-Epi Gen III molecular beam epitaxy chamber: The absorbing layer was unintentionally doped, with an estimated residual n-type carrier concentration of $\sim 10^{16}$ $cm^{-3}$, and the barrier layer was estimated to have residual p-type carrier concentration of $\sim 10^{15}$ $cm^{-3}$. The doping values were obtained on separate samples specifically grown for Hall measurements. Triple axis X-ray diffraction patterns exhibited sharp peaks for the bulk InAsSb layers with FWHM less than 45 arcsec and clear Pendellosung fringes from the barrier. After growth, the absorption coefficient, the band gap and the minority carrier lifetime of the superlattice were measured using absorption spectroscopy, photoluminescence (PL) and optical modulation response [14] (OMR), respectively (Figs. 2 and 3). The absorption QE was found from the ratio of the transmissions measured for two samples from the same epi-wafer. The first sample is the detector structure with absorber intact. In the second sample the absorber layer was completely etched away so transmission through it provides an estimate of the substrate absorption. We observe that substrate absorption is high across 2–6 μm spectral region studied here (not shown) so the responsivity $QE_{resp}$ measured in our experiment is for single pass only. The substrate absorption is high in this subbandgap photon energy region because of the free carrier absorption. The measured minority carrier lifetime is $\tau \approx 300$ ns in the temperature range $T = 77$–$200$ K and becomes shorter at higher temperature reaching the value of $\tau \approx 100$ ns at $T = 325$ K (Fig. 3).

Standard optical lithography (contact mode) was used to define the patterns for square mesas of area $4 \times 10^4$ $\mu m^2$. After pattern development, the wafer was etched in a citric acid based wet chemical etching solution to isolate individual devices. The etching depth was approximately 2 μm, resulting in etching into bottom of the absorber and full delineation of single pixel detectors.

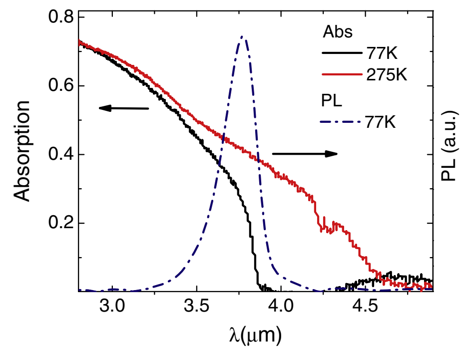


**Fig. 2.** Absorption quantum efficiency $QE_{abs}$, at $T = 77$ K and 275 K, and photoluminescence (PL) signal at $T = 77$ K.

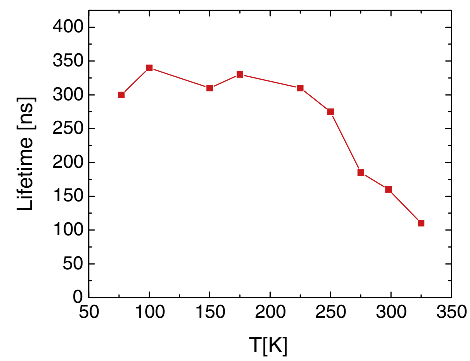


**Fig. 3.** Minority carrier (hole) carrier lifetime vs. temperature.

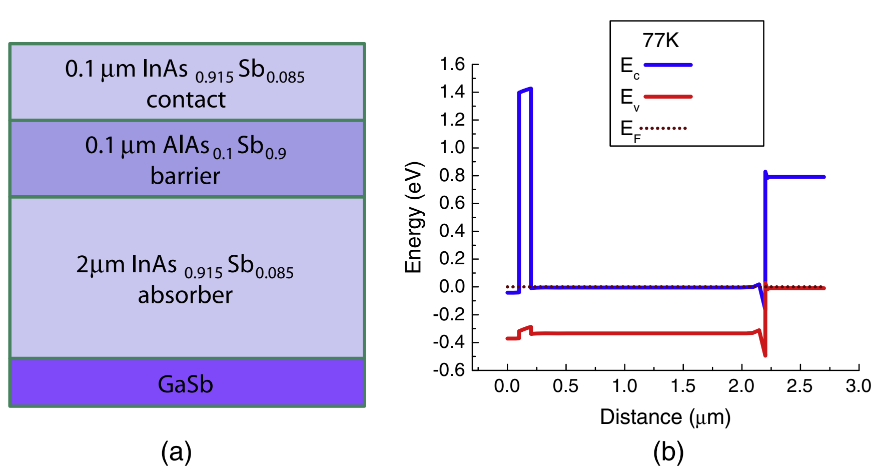


**Fig. 1.** (a) Growth sequence of the nBn photodetector which consists of absorber region consists of a 2 μm thick $InAs_{0.915}Sb_{0.085}$ absorber followed by a 0.1 μm $AlAs_{0.1}Sb_{0.9}$ barrier and a 0.1 μm $InAs_{0.915}Sb_{0.085}$ top contact and (b) energy band diagram of nBn detector at zero applied bias for temperatures $T = 77$ K.

Please cite this article in press as: A. Soibel et al., Room temperature performance of mid-wavelength infrared InAsSb nBn detectors, Infrared Phys. Technol. (2014), http://dx.doi.org/10.1016/j.infrared.2014.09.030